SUPPLEMENTARY DATA

Heterochromatin Protein 1 alpha: a hallmark of cell proliferation relevant in clinical oncology

DE KONING Leanne, SAVIGNONI Alexia, BOUMENDIL Charlène, REHMAN Haniya, ASSELAIN Bernard, SASTRE-GARAU Xavier, ALMOUZNI Geneviève

Supplementary figure legends:

Supplementary figure S1: HP1α levels progressively increase after exit from quiescence. **A.** BJ primary fibroblasts are arrested in quiescence (G0) by serum starvation and released by adding back serum for the indicated time period. Total protein levels are analyzed by Western blot. CAF-1 p60 (Polo et al, 2004) and Cyclin A are used as markers for cell proliferation. β-actin is used as a loading control. ***B***. Flow cytometry analysis of the cell cycle distribution of the cells shown in *A*.

Supplementary figure S2: HP1α expression does not visibly vary during the cell cycle. ***A***. HeLa cervical carcinoma cells are synchronized in the cell cycle by release from double thymidine block (G1, G1/S, S, G2) and by nocodazole (M). Total protein extracts are analyzed for HP1α expression levels using Western Blot. β-actin is used as a loading control and Cyclin A as a marker for G2/S phases. CAF-1 p60 is shown for comparison. ***B***. Flow cytometry cell cycle analysis of the synchronized cells used in *A*. ***C***. BJ foreskin primary fibroblasts are synchronized in the cell cycle by release from double thymidine block (G1, G1/S, S, G2) and by nocodazole (M). HP1α protein levels are analyzed in total cell extracts by Western Blot. β-actin is used as a loading control and Cyclin A as a marker for G2/S phases. CAF-1 p60 is shown for comparison. ***D***. Flow cytometry analysis of the cell cycle distribution of the synchronized cells shown in *C*. ***E***. HP1α mRNA levels in synchronized BJ cells, as determined by quantitative RT-PCR. Levels are normalized to the reference gene ribosomal protein P0-like protein (RPLPO) (de Cremoux et al, 2004) and levels in asynchronously proliferating cells are set to 100%. CAF-1 p60 and CAF-1 p150 levels are shown for comparison (Polo et al, 2004). Error bars represent data from two independent experiments.

Supplementary figure S3: Levels of HP1 proteins in soluble and chromatin-bound nuclear fractions. ***A.*** Scheme depicting the extraction procedure to obtain soluble and chromatin-bound nuclear fractions of the breast cancer cell line Hs578T (T) and the healthy mammary cell line Hs578Bst (Bst), which are derived from the same patient (Hackett et al, 1977). ***B.*** HP1α, β and γ protein levels are analyzed by Western Blot in soluble and chromatin-bound nuclear extracts from the cancer cells Hs578T (T) and the healthy cells Hs578Bst (Bst). Loading was corrected in a manner to deposit an identical amount of cells ($2x10^5$ and $4x10^5$ cells for each extract). We revealed several classical loading controls. While the fractionation of α-tubulin and the presence of β-actin differ slightly between tumoral and healthy cells, GAPDH reflects best the identical loading under these experimental conditions. Cyclin A and CAF-1 p60 are shown for comparison.

Supplementary figure S4: Nuclear distribution of HP1α, but not H3K9me3, is altered in breast cancer cells compared to healthy mammary cells. ***A***. Immunofluorescence staining of HP1α in the breast cancer cell line Hs578T (T) and in the non-tumoral mammary cell line Hs578Bst (Bst). Costaining for centromeres, using CREST patient serum, reveals a partial although incomplete colocalization with the HP1α spots in Hs578T breast cancer cells. DNA is stained with DAPI. Indicated below the microscopy images are the mean percentages of cells showing clearly distinguishable HP1α spots in the breast cancer cell line Hs578T (T) and in the healthy mammary cell line Hs578Bst (Bst). Standard error, based on two independent experiments, is indicated. **B.** Nuclear distribution of the H3K9me3 histone modification, compared to HP1α in the tumoral (T) and non-tumoral (Bst) mammary cells. DNA is revealed with DAPI. **C.** Costaining of HP1α with Cdt1 (indicative for G1 phase), Cyclin A (indicative for S and G2 phase), or histone H3 phosphorylated on S10 (H3S10P; indicative for G2 and M phase), does not reveal a correlation between cell cycle status and spotted HP1α patterns. Scale bars: 10 μm.

Supplementary figure S5: Downregulation of HP1α in primary cells affects (pro)metaphase. ***A.*** BJ primary fibroblasts are transfected by nucleofection with control siRNA (siGFP) or two different siRNA sequences targeting HP1α (α.1 or α.3). Total protein levels are analyzed by Western blot. HP1β and HP1γ are revealed to show the specificity of the siRNA for the HP1α isoform. ***B.*** Flow cytometry analysis of the cell cycle distribution of cells shown in *A*, 72 hours after transfection with control siRNA (siGFP) or two different

siRNA sequences targeting HP1α (siHP1α.1/3). ***C***. Profiles of mitotic cells are analyzed by immunofluorescence 72h after transfection. Enrichment in mitotic cells is achieved by a 6 hours release from a 12h thymidine block. Depicted are typical mitotic profiles (upper panel) and the presence of each mitotic phase as a percentage of the total number of mitotic cells (graph). Error bars represent standard errors, based on three independent experiments (n>100 for each) of which two were blind counted. **D.** Time of mitosis after two subsequent transfections with control siRNA (siGFP) or HP1α siRNA (siHP1α.3), as determined by live cell imaging. DNA is visualized by expression of H2B-Cherry (red). Images were acquired every 20 minutes for a period of 24h, starting 48h after the second transfection. The time of mitosis (upper graph) was defined as the time between the condensation of DNA and the establishment of two distinct cells. The average number of images depicting mitotic cells in (pro-)metaphase, before the onset if chromosome segregation, was also determined (lower graph). Means of three independent experiments are depicted, representing a total number of 130 and 87 mitotic cells for siGFP and siHP1α, respectively. P-values were determined with a test of Mann-Whitney Wilcoxon. Mean H2B-cherry transfection efficiencies were 37% and 39% for siGFP and siHP1α, respectively.

Supplementary figure S6: HP1α mRNA is overexpressed in multiple types of cancer and correlates with clinical and molecular data. ***A.*** Boxplot representation of microarray expression profiles of HP1α in different types of cancer (red/green) compared to normal tissue (blue). Boxes represent the 25th-75th percentile; brackets: range; black line: median; black dots: outliers; n: sample number. p-values are based on Student's T-test. Results are analyzed and plotted using ONCOMINE (Rhodes et al, 2004), and exploit data from transcriptome studies on different tumor types (Andersson et al, 2007; Pyeon et al, 2007; Quade et al, 2004; Ramaswamy et al, 2003; Richardson et al, 2006; Yu et al, 2004). ***B.*** *Left panel:* Correlation of HP1α expression levels with the time to relapse in childhood acute lymphoblastic leukemia (Kirschner-Schwabe et al, 2006). Relapse occurs very early (within 18 months after initial diagnosis), early (>18 months after initial diagnosis but <6 months after cessation of frontline treatment) or late (>6 months after cessation of frontline treatment). Boxplot representation as in *A*. *Right panels:* Scatter plot representation of the positive correlation of HP1α expression levels with CAF-1 p150 and the proliferation marker Ki67 expression levels in childhood acute lymphoblastic leukemia (Kirschner-Schwabe et al,

2006). Red line: line of best fit; R: Pearson's correlation coefficient. Results are analyzed and plotted using ONCOMINE (Rhodes et al, 2004).

Supplementary figure S7: Overexpression of HP1α in human tumor samples is detected with a polyclonal antibody and is not accompanied by altered H3K9me3 staining. A. Immunohistochemistry staining, using a polyclonal HP1α antibody, of a tissue array containing frozen human tissue sections from tumoral and healthy origin. Tissues were counterstained with hematoxylin. **B.** A frozen human tissue array (same batch as in A.) is stained for H3K9me3 by immunohistochemistry and counterstained with hematoxylin. Scale bars: 50 μm.

A. **Total protein**

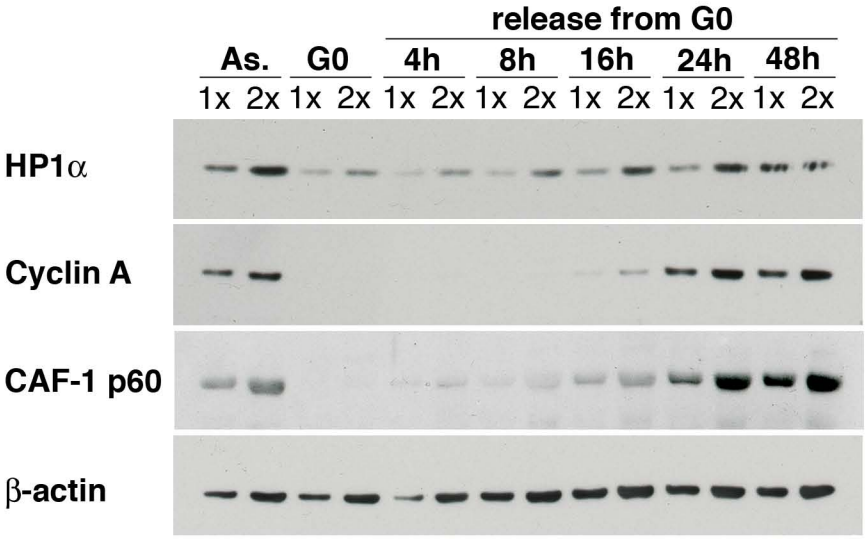

B. **Flow Cytometry**

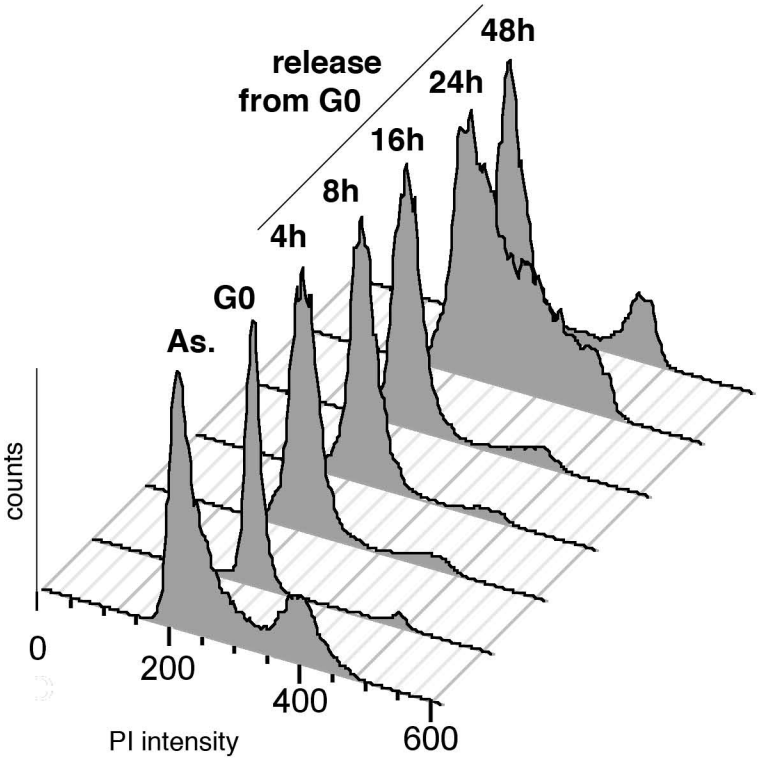

Supplementary figure S1

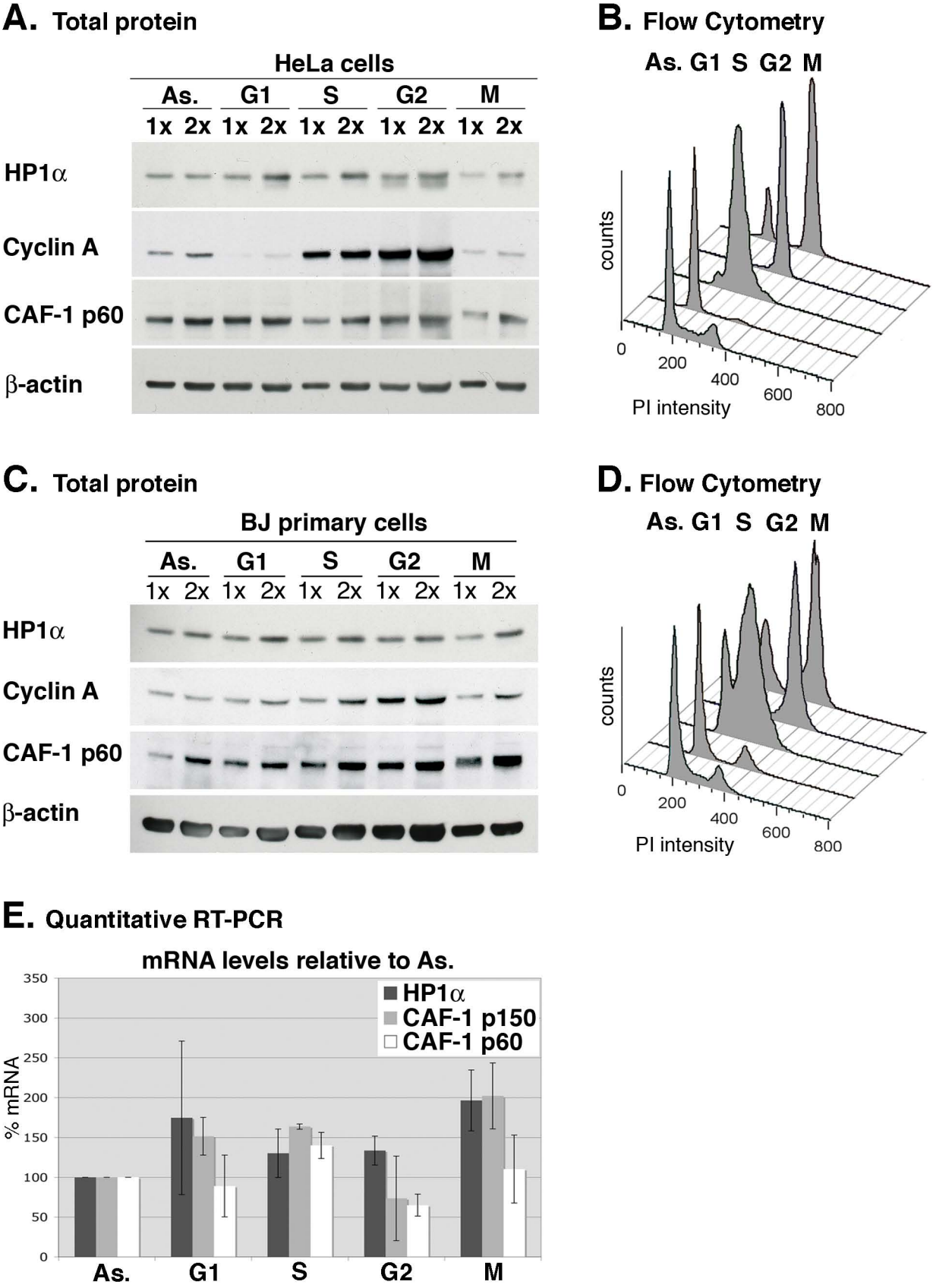

Supplementary figure S2

A. Extraction procedure

T: Tumoral cells (Hs578T)
Bst: Non-tumoral cells (Hs578Bst)

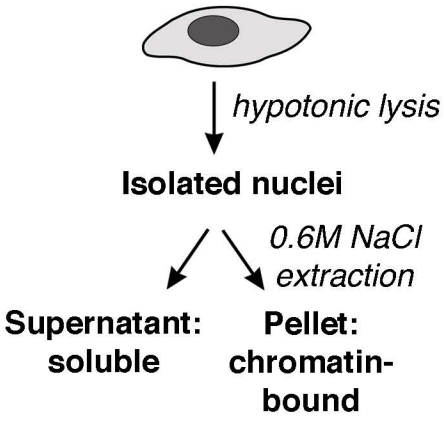

B. Western Blot

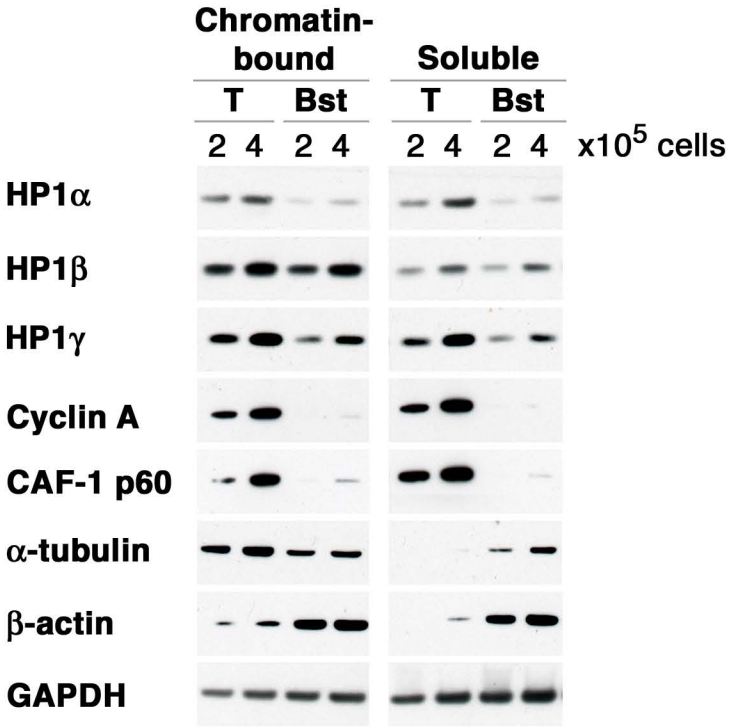

Supplementary figure S3

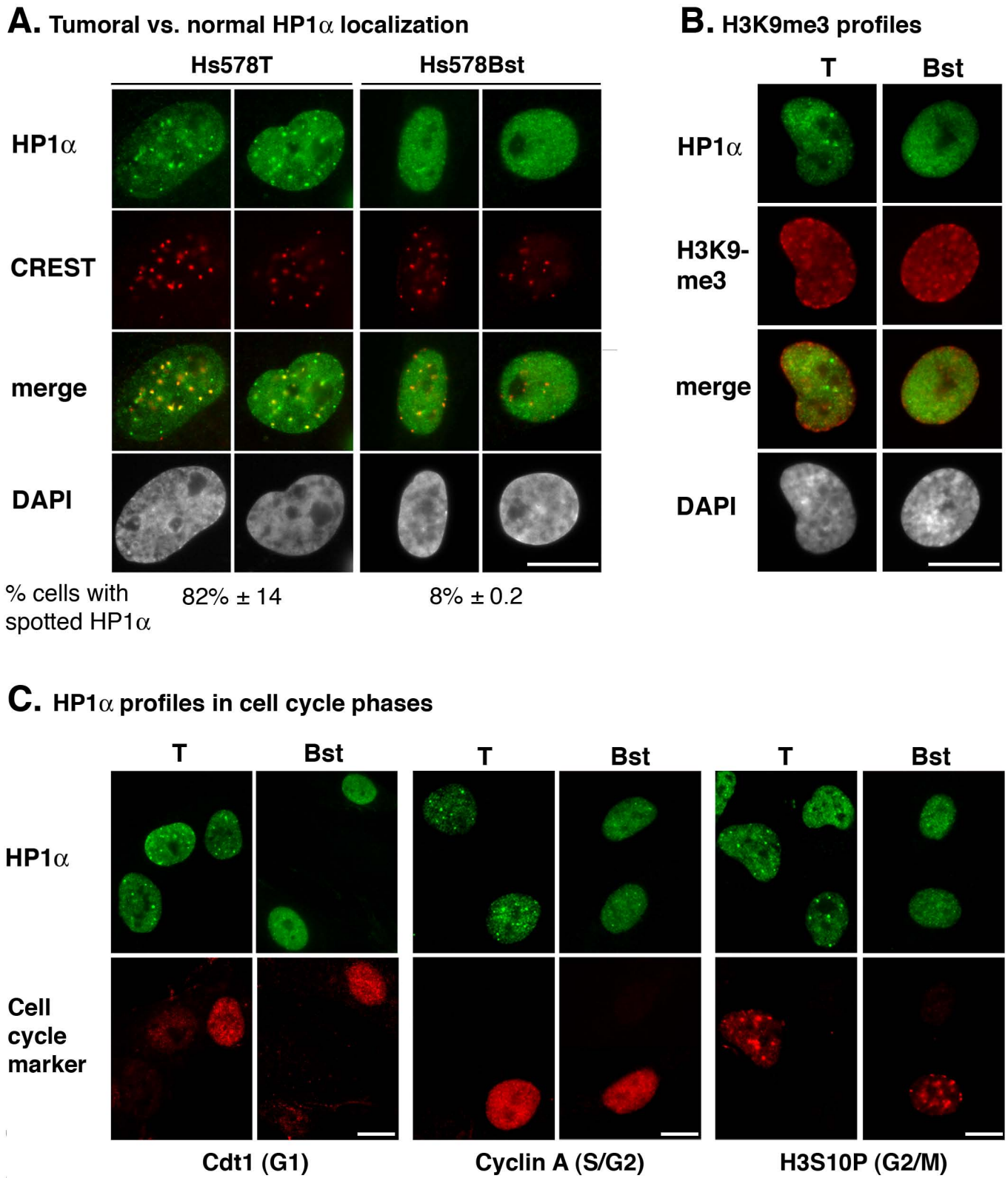

Supplementary figure S4

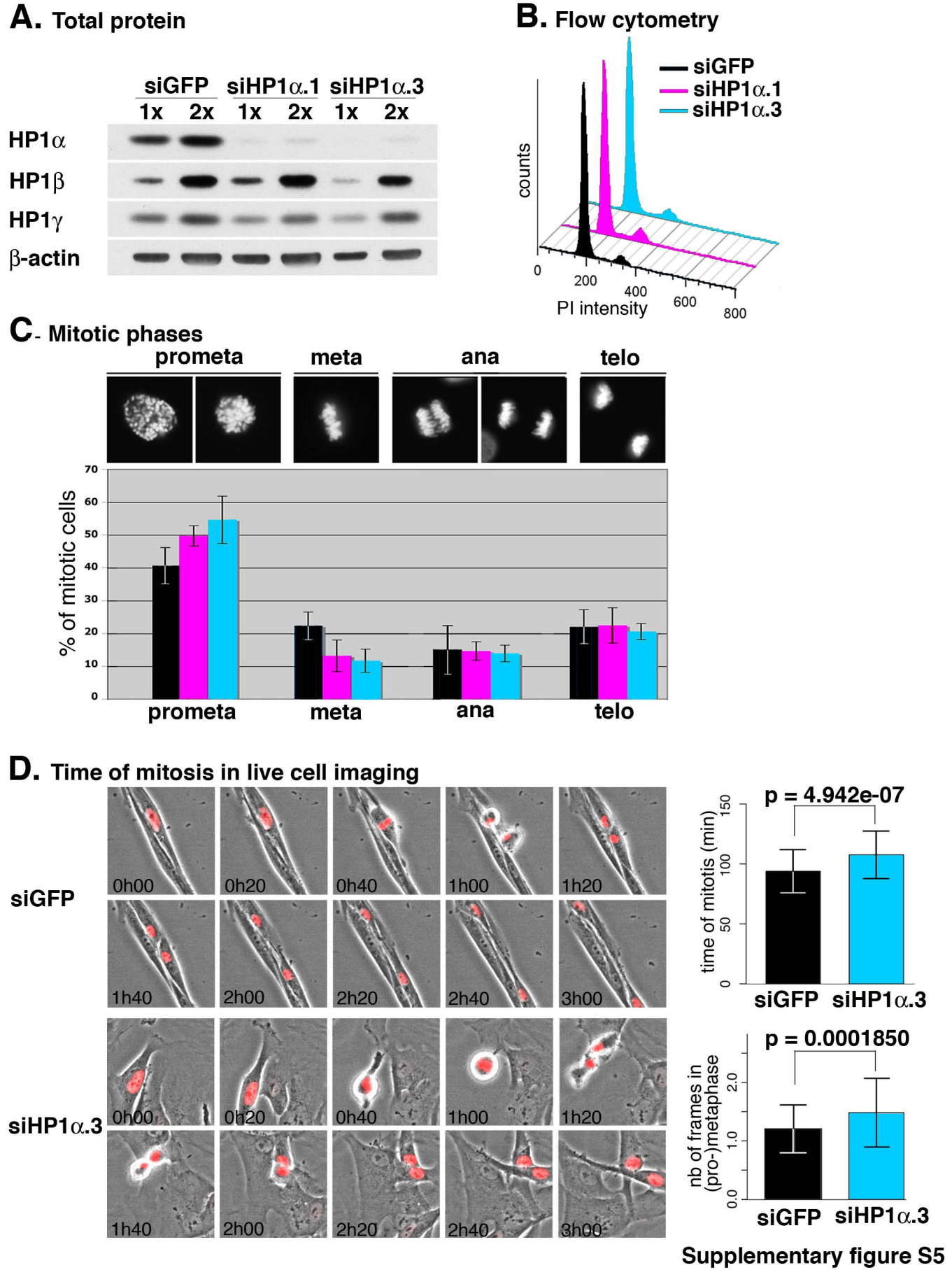

Supplementary figure S5

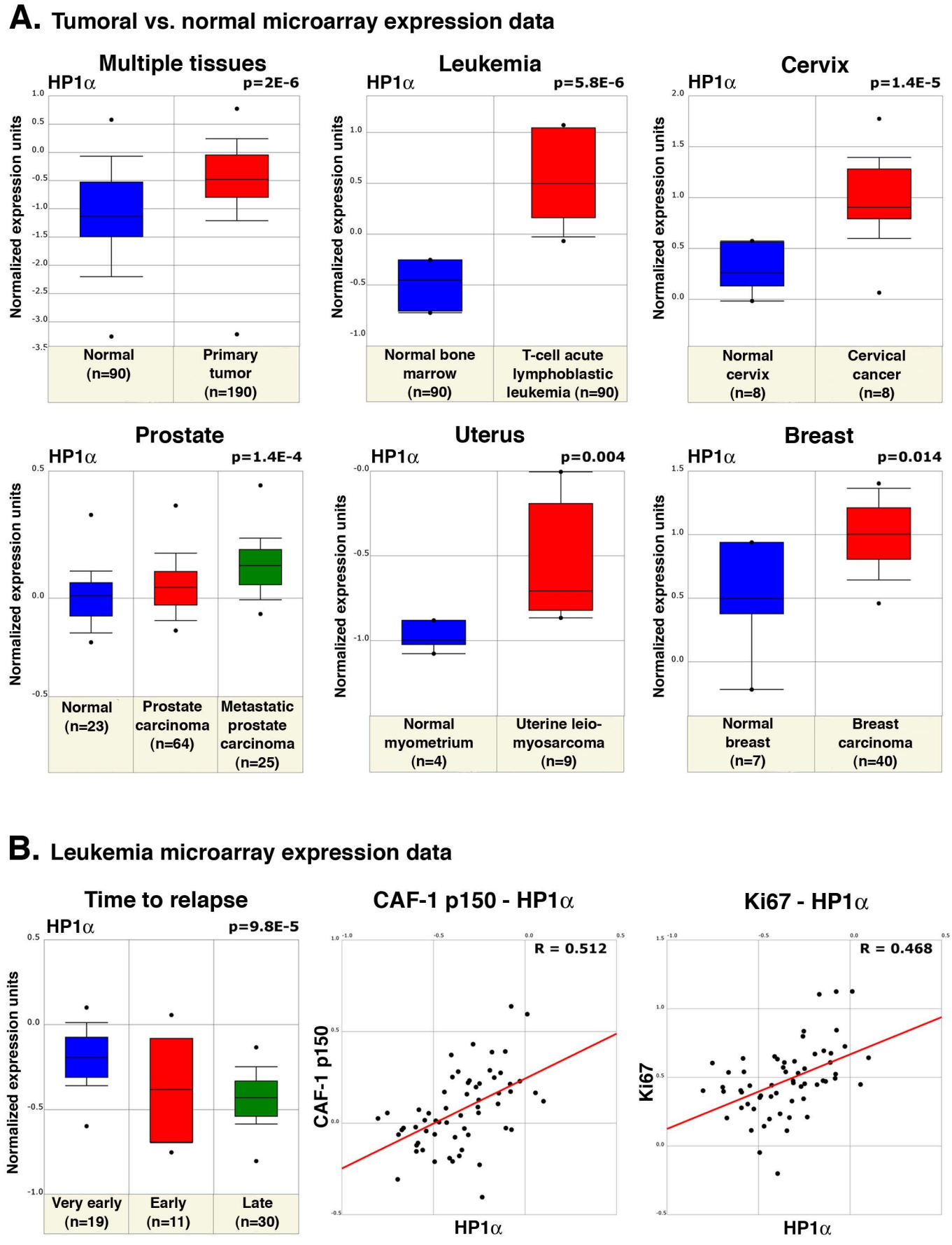

Supplementary figure S6

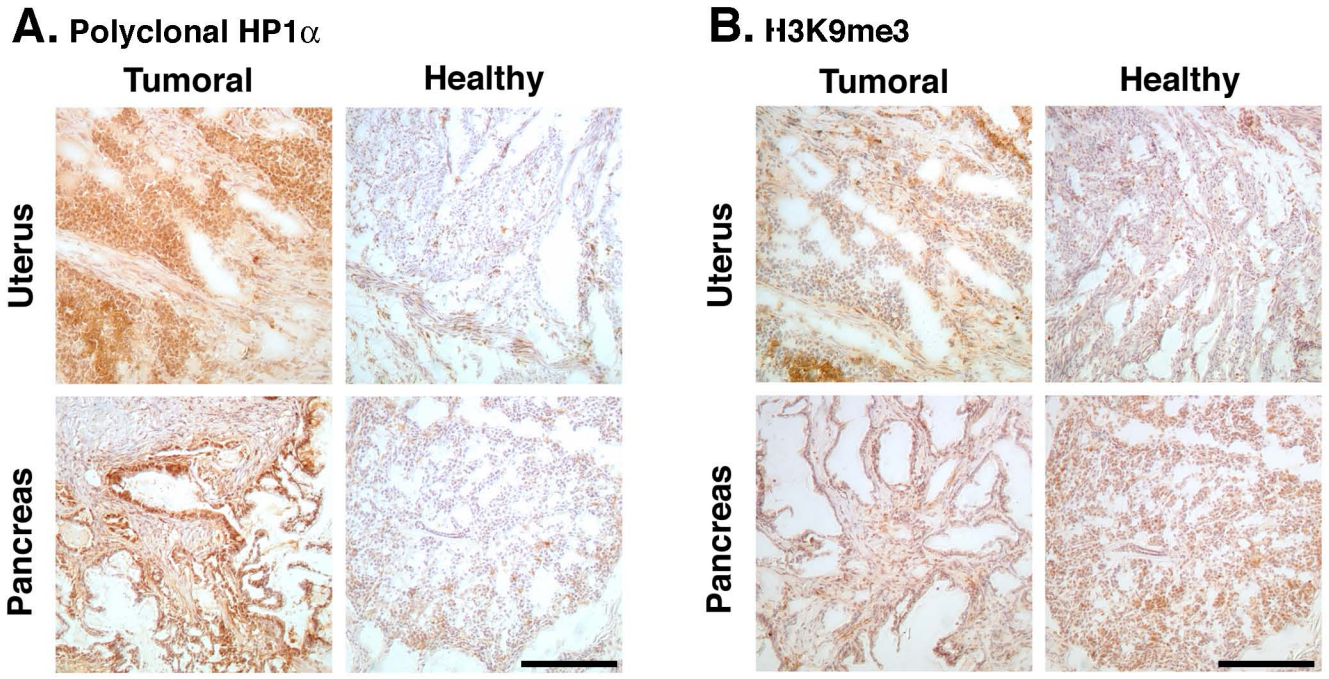

Supplementary figure S7

Table I: Description of the patient samples		
Age	median: 53 (range: 26-70)	
Menopaused	yes	54%
	no	46%
Histological type	ductal	88%
	lobular	9%
	papillary	1%
	tubular	1%
Size classification	T0/T1	62%
	T2	38%
Tumor size (mm)	median: 18 (range: 6-50)	
Grade EE	I	33%
	II	42%
	III	25%
Estrogen receptor	positive	86%
	negative	14%
Progesteron receptor	positive	69%
	negative	31%
Mitotic index	median: 8 (range: 0-105)	
Ki67	<= 15	52%
	15 - 40	24%
	> 40	24%
Adjuvant chemotherapy	no	93%
	yes	7%